Meat and Muscle Biology™

Color Stability and Tenderness Attributes of Beef *Longissimus Lumborum* Steaks at 2 Different Aging Periods Are Impacted by Metabolic Characteristics

Jade V. Cooper[1], D. Andy King[2]*, Steven D. Shackelford[2], Peg Ekeren[2], Carol L. Lorenzen[3], and Tommy L. Wheeler[2]

[1]Division of Animal Sciences, University of Missouri, Columbia, MO 65211, USA
[2]USDA–ARS, Roman L. Hruska US Meat Animal Research Center, Clay Center, NE 68933, USA
[3]Department of Animal and Rangeland Sciences, Oregon State University, Corvallis, OR 97331, USA
*Corresponding author. Email: andy.king@usda.gov (D. Andy King)

Abstract: Beef color and tenderness are 2 of the most important attributes contributing to the perception of meat quality and palatability. Studies in search of biomarkers explaining mechanisms regulating meat color stability and tenderness have identified biology in common with both traits. Therefore, the objective of this study was to evaluate the contribution of metabolic factors to animal variation in beef *longissimus lumborum* tenderness and color stability. Beef carcasses ($n = 96$) were selected based on tenderness and color stability predictions at grading. *Longissimus lumborum* muscles were obtained from both sides of each carcass and aged until 12 or 26 d postmortem. Overall tenderness ratings, slice shear force, desmin degradation, and sarcomere length were used to characterize tenderness. Instrumental color values measured during simulated retail display, oxygen consumption, and nitric oxide metmyoglobin-reducing ability were used to characterize color stability. Metabolic traits including pH, glycolytic intermediates, proportion of Type I fibers, sarcoplasmic and myofibrillar carbonyls, and myoglobin concentration were determined on each muscle. Relationships of metabolic traits to tenderness and color stability were assessed with correlation analysis, analysis of variance across clusters derived from tenderness and color stability data, and principal component analysis. Increased nitric oxide metmyoglobin-reducing ability was associated with decreased ($P < 0.05$) tenderness ratings and desmin degradation and longer sarcomere lengths. Oxygen consumption was associated with decreased tenderness ratings and increased slice shear force ($P < 0.05$). Both tenderness and lean color stability were negatively related to increased oxidative metabolism. These results indicated that relationships exist between tenderness and lean color stability. Moreover, animal variation in both tenderness and color stability is influenced by muscle metabolism.

Key words: beef, color, longissimus lumborum, metabolism, tenderness
Meat and Muscle Biology 9(1): 18387, 1–18 (2025) **doi:10.22175/mmb.18387**
Submitted 28 September 2024 Accepted 12 December 2024

Introduction

Color is the primary indicator of freshness and quality of beef at the consumer point of purchase (Mancini and Hunt, 2005). Deviations from acceptable color can lead to consumer discrimination and refusal to buy products. Beef lean color and color stability have been reported to be impacted by numerous factors that are also associated with muscle metabolism including ultimate pH (McKeith et al., 2016; Page et al., 2001; Zhang et al., 2018), myoglobin (Suman and Joseph, 2013; Wang et al., 2021) mitochondrial abundance and functionality (McKeith et al., 2016; Mitacek et al., 2019; Ramanathan et al., 2021), metmyoglobin-reducing activity (Bekhit and Faustman, 2005; King et al., 2011; McKenna et al., 2005; Sammel et al., 2002), and oxygen consumption (King et al., 2011; Tang et al., 2005). The complexity of the interactions among the multitude of metabolic factors affecting beef lean color and color stability require additional scrutiny.

Historically, tenderness has primarily been deemed the most important palatability trait for consumer eating satisfaction. Consumers have indicated they are willing to pay premiums for guaranteed tender beef products. Beef tenderness is impacted by a variety of intrinsic factors such as the ultimate pH of muscle (Grayson et al., 2016; Maddock et al.; 2005, Watanabe et al., 1996), sarcomere length (King et al., 2003, Koohmaraie et al., 2002), postmortem aging time and proteolysis extent (Huff-Lonergan et al., 1996; Koohmaraie, 1996; Taylor et al., 1995) and oxidation (Malheiros et al., 2019; Rowe et al., 2004). Although these factors have been proven to impact beef tenderness, they do not fully explain tenderness development and variability (Shackelford et al., 2012a). As tenderness plays such a crucial role in consumer eating satisfaction, a more in-depth understanding of tenderness and the mechanisms behind it is of great importance.

The advent of technologies that enable the profiling of the metabolome and proteome of skeletal muscle and its constituents has facilitated a greater understanding of the molecular signatures associated with variation in meat quality phenotypes. Such proteomics and metabolomics work in both color and tenderness studies have indicated that specific proteins and metabolites associated with various biological and metabolic pathways are correlated with beef color stability (Canto et al., 2015; Joseph et al.; 2012, Nair et al., 2018; Nair et al., 2016; Ramanathan et al., 2020a; Ramanathan et al., 2020b; Suman et al., 2006) and beef tenderness traits (Antonelo et al., 2020; D'Alessandro et al., 2012; Gagaoua et al., 2019; King et al., 2019; Picard et al., 2018; Picard et al., 2014). Many of these pathways and their products have reported associations with both color stability and tenderness attributes, which indicates the potential for both antagonisms and synergies that must be addressed in management to optimize meat quality.

Biomarkers identified by proteomic and metabolomic investigations of meat quality attributes will be beneficial in elucidating the mechanisms underlying animal variation in these traits and developing strategies to optimize both color stability and tenderness in a systems approach; however, these biomarkers need to be validated in multiple, independent sample sets to confirm their suitability for that purpose. Therefore, the objectives of this study were to characterize the relationships between beef *longissimus lumborum* tenderness and lean color stability and to describe the contributions of metabolic factors to variation in beef *longissimus lumborum* lean color stability and tenderness.

Materials and Methods

Carcasses used in this experiment were selected and obtained postmortem from a commercial facility inspected by the United States Department of Agriculture Food Safety and Inspection Service. Therefore, animal care and use approval was not obtained for this experiment.

Sample selection and fabrication

Beef carcasses (A maturity; $n = 96$) were selected for this experiment on 4 selection days ($n = 24$ each day) At grading (approximately 24 h postmortem), an image-analysis-based grading system (VBG 2000 GigE, Oranienburg, Germany) was used to collect carcass grade characteristics (Shackelford et al., 2003) and screened for predicted tenderness using an algorithm developed for the VBG 2000 Gig E system (S. D. Shackelford, personal communication May 15, 2019) and for predicted color stability using an algorithm (D. A. King, personal communication June 10, 2019) developed for the USMARC VIS/NIR non-invasive tenderness prediction system (Shackelford et al., 2012b). Carcasses were selected to be above and below arbitrary thresholds for predicted slice shear force (tough >15 kg; tender < 15 kg) and predicted overall color change (ΔE; stable <8; labile > 8). Six carcasses fitting each combination of predicted color stability and predicted tenderness classes were selected on each sampling day to ensure adequate variation in the 2 traits of interest and to facilitate the study of factors contributing to the variation in both traits.

The beef, loin, and strip loin, similar to Institutional Meat Purchase Specifications #180, (USDA, 2014) from both sides of each carcass, were blocked and assigned to an aging period of 12 or 26 d postmortem so that each aging time and carcass side combination was represented equally in each predicted color and tenderness class. A thin steak (12 mm) was removed from the anterior face of the subprimals and used for 48-h pH determination. Subprimals were vacuum packaged, sorted by aging time, boxed, and transported to the US Meat Animal Research Center abattoir via refrigerated truck (−2°C), and wet aged at 1°C for the designated period.

After aging, the *longissimus lumborum* was trimmed free of external fat and accessory muscles and cut into 28-mm-thick steaks using a Grasselli NSL400 (Grasselli-SSI, Throop, PA, USA). Steaks ($n = 4$) were placed in simulated retail display, used for slice shear force determination, used to measure

nitric oxide metmyoglobin-reducing ability and oxygen consumption, or designated for laboratory analyses. Additional steaks ($n = 2$) were vacuum packaged and frozen at −20°C for use with a trained sensory panel.

Simulated retail display

Steaks were placed on a polystyrene tray lined with a soaker pad and overwrapped with oxygen-permeable polyvinylchloride film (stretchable meat film 55003815; Prime Source, St Louis, MO, USA; Oxygen transmission rate = 1.4 mL/[$cm^2 \times 24$ h] at 23°C). Steaks were exposed to continuous fluorescent lighting (3500 K color temperature; CRI = 86; 32W; T8 Ecolux bulb model no. F32T8/SPX35, GE, GE Lighting, Cleveland, OH, USA) for an 11-d period. Light intensity at the steak surface was approximately 2000 lx. Simulated retail display occurred at approximately 1°C and no temperature fluctuations due to defrosting were encountered.

Two hours were allotted to allow steaks to oxygenate before initial color (d 0) measurements were obtained. Duplicate color readings were taken using a Hunter MiniScan XE Plus Colorimeter (HunterLab, Reston, VA, USA) equipped with a 25-mm port set to collect spectral data with Illuminant A and a 10° observer. Color data, including Commission Internationale de l'Éclairage (CIE) color space values (L^*, a^*, and b^*), chroma, hue angle, and overall color change (ΔE), was collected on days 0, 1, 4, 7, and 11 of simulated retail display (King et al., 2023). The instrument was calibrated as prescribed by the manufacturer before each data collection session.

pH and myoglobin concentration

Muscle pH was determined on samples removed from the strip loins at 48 h postmortem and after aging (ultimate pH) using the iodoacetate method (Bendall, 1973). A Corning 125 pH meter equipped with a semi-micro combination electrode (Corning, Inc. Corning, NY, USA) that had been calibrated using pH 4 and 10 standards was used to measure muscle pH.

Myoglobin content determination was conducted using the method described by King et al. (2023) with modification. A powdered sample (2.5 ± 0.05 g) was extracted with 25 mL of cold 40 mM potassium phosphate buffer. After centrifugation for 35 min at 15,000 × g (4°C), supernatants were filtered using a syringe filter (Nalgene surfactant-free cellulose acetate membrane .45 µm). Absorbance spectra were collected at 525 and 700 nm using a Spectramax plus 96-well plate reader (Molecular Devices, Sunnydale, CA, USA). Myoglobin content was calculated using equations provided by King et al. (2023).

Nitric oxide metmyoglobin-reducing ability and oxygen consumption

For nitric oxide reducing activity and oxygen consumption (OC), a 2.54 cm × 2.54 cm × steak thickness cube from the center of each steak as described by (King et al., 2023). Cubes were then divided in half along the steak thickness dimension to expose the interior portion of the muscle, which was used for oxygen consumption, whereas the previously exposed surface was used for nitric oxide metmyoglobin-reducing ability. Samples used for nitric oxide metmyoglobin-reducing ability were oxidized in 50 ml of 0.3% sodium nitrite solution for 30 min at 20°C as described by King et al. (2023). Samples were removed, vacuum packaged, and immediately scanned with a Hunter MiniScan colorimeter through the vacuum packaging film with settings as previously described. The instrument was calibrated through the vacuum packaging film. Samples were held at 30°C for 2 h before being scanned again with identical settings as the initial scan. Equations provided by King et al. (2023) were used to quantify surface metmyoglobin.

Oxygen consumption was determined by methods described in King et al. (2023). The newly exposed surface of the bottom portion of the cube was covered with oxygen-permeable film and allowed to oxygenate for 2 h (4°C). Oxygenated samples were individually vacuum packaged and immediately scanned with a Hunter MiniScan. Vacuum-packaged samples were incubated for 20 min at 25°C and rescanned with the colorimeter. Proportion of surface oxymyoglobin on the deoxygenated and oxygenated samples was determined and oxygen consumption was reported as the percentage decrease in surface oxymyoglobin.

Trained sensory panel analysis

On each day of sensory panel evaluation, panelists were presented samples from each of the prediction classes and the presentation order of the pH classes was blocked across sensory evaluation days. Samples were thawed at 5°C for 24 h before being cooked on a conveyorized grill (model TBG-60 Magigrill [MagiKitch'n Inc., Quakertown, PA, USA]) as described by Wheeler et al. (1998) to target a final internal temperature of 70°C (after post-cooking temperature rise) immediately prior to presentation to panelists. Internal steak temperatures were monitored

pre- and post-cooking with a handheld thermometer equipped with a thermocouple probe (Cole-Parmer, Vernon Hills, IL, USA) placed in the geometric center of the steak. Once cooking was complete, exterior fat and connective tissue were discarded and steaks were cut into 1.37 cm × 1.37 cm × steak thickness cubes. Cubes were mixed and then randomly presented, in triplicate, to each panelist. On each panel day, panelists were given a warm-up sample before formal evaluation began. A highly experienced descriptive attribute panel trained in accordance with guidelines provided by (Cross et al., 1978) and (AMSA, 2016). Overall tenderness and juiciness were rated on an 8-point scale (1 = extremely tough or dry, 8 = extremely tender or juicy).

Slice shear force

Steaks utilized for slice shear force (SSF) were fresh (never frozen) and equilibrated to 5°C for approximately 24 h before cooking. Cooking was done as described above to achieve an internal temperature of 70°C. Shear force values were determined using methods described in Shackelford et al. (1999). Internal steak temperatures were monitored as described above. A 1-cm-thick, 5-cm-long slice was removed from each cooked steak parallel to muscle fibers. Slices were sheared with an electronic testing machine (TMS-PRO Texture Measurement System, Food Technology Corp, Sterling, VA, USA) equipped with a slicer force blade and a crosshead speed of 500 mm/min. Slice shear force values are reported in kg.

Sarcomere length determination

Sarcomere length was determined using the helium-neon laser diffraction method described by Cross et al. (1981). Cooked slices from slice shear force determination were trimmed of all hard, cooked edges from each slice. These samples were finely diced and snap-frozen in liquid nitrogen then pulverized to a fine powder and stored at −20°C until analyzed.

A small amount of powdered tissue was placed on a microscope slide. Approximately 100 µl of sucrose buffer (0.2 M Sucrose in 0.1 M $NaHPO_4$, pH 7.4) was added to the sample. Six diffraction patterns were identified and traced onto a single piece of paper for each of the 6 aliquots of each sample. A total of 36 diffraction patterns were scanned into JPEG images and Image Pro software (Media Cybernetics, Inc., Rockville, MD, USA) was used to measure the diffraction bands, and sarcomere length was calculated as described by Cross et al. (1981).

Desmin degradation and myosin heavy chain isoforms

A whole muscle extract prepared from frozen powdered tissue described above was used to quantify desmin degradation and the proportion of myosin heavy chain (MHC) isotypes. For desmin degradation, 1 gram of frozen, powdered sample was homogenized in 10 volumes of TRIS-EDTA buffer (tris[hydroxymethyl] aminomethane-Ethylenediaminetetraacetic acid) for 20 s using a Polytron at setting #4 (Kinematica Polytron™ PT 2100 Homogenizer, Kinematica, Inc, New York, NY, USA). A 0.5-ml aliquot of homogenized sample was transferred to a 1.5-ml microcentrifuge tube. Then, 0.5 ml of 2× treatment buffer, pH 6.8 (0.125 M Tris, 4% EDTA, 20% glycerol, water) was added to the sample tube, and samples were incubated in a 50°C water bath for 20 min. Mixing was repeated and samples were reheated for an additional 5 min. Samples were centrifuged for 20 min at 16,000 × g to pellet insoluble material and protein concentration was determined on the supernatant using Pierce micro-BCA Protein Assay Kit (Thermo Scientific, Waltham, PA, USA). Samples were diluted to 0.3 mg/ml in 0.1× sample buffer. Sample buffer was made from the 10× sample buffer supplied in the Protein Simple, Simple Western 12-230 kDa Separation Module (Bio-Techne/Protein Simple, San Jose, CA, USA).

Percent desmin degradation was determined using the Simple Western Automated Western Blot System utilizing the Wes instrument (Bio-Techne/Protein Simple, San Jose, CA, USA). Samples (0.3 mg/ml) were prepared using the WES kits as prescribed by the manufacturer. Samples collected from *longissimus lumborum* muscles at 0 h postmortem were prepared as described previously and used as a standard for zero desmin degradation. Samples were prepared using the protocol supplied with the 12–230 kDa Separation module. The assay also used the Protein Simple Anti-Rabbit Detection Module. Primary antibody (Rabbit monoclonal desmin, clone RM234, Novus Biologicals, Centennial, CO, USA) was then diluted (1:50) and immediately stored on ice. Immediately prior to starting the assay, the luminol-peroxide solution was made by combining 200 µl of peroxide solution and 200 µl of luminol supplied in the WES assay kit. The secondary antibody used was the anti-rabbit secondary antibody supplied in the

Protein Simple Anti-Rabbit Detection Module (Bio-Techne/Protein Simple, San Jose, CA, USA). After pipetting the sample and assay solutions into the supplied plate, the plate was centrifuged at 1000 × g for 5 min. The plate was placed into the WES system and a new capillary cartridge was inserted into the cartridge holder. The WES system was started and run until completion. The WES system software (Compass for Simple Western) generated a curve representing the levels of desmin in each sample. Percent desmin degradation was determined by normalizing the data to triplicate 0-h postmortem samples (collected from carcasses not included in the present experiment) run on each plate. Each peak was individually evaluated to ensure desmin degradation was correctly accounted for in each sample.

Myosin heavy chain isoforms were separated and quantified using methods described in Picard et al. (2011) with modifications. A separate whole muscle extract from raw *longissimus lumborum* tissue was prepared using the protocol described previously for desmin degradation with the exception that samples were diluted to final concentration (0.3 mg/ml) with 2 × treatment buffer, pH 6.8 (0.125 M Tris, 4% EDTA, 20% glycerol; pH = 6.8) containing 5% 2-mercaptoethanol and 0.8% bromophenol blue.

Bio-rad Mini-Protean gels (Bio-Rad, Hercules, CA, USA) were poured with a 6% stacking (30% acrylamide [50:1], 0.04% sodium dodecyl sulfate (SDS), 47% glycerol, 6 mM EDTA, 115 mM glycine, 110 mM Tris [pH 6.7], H_2O, 0.1% ammonium persulfate (APS), 0.05% TEMED) and a 9% separating (30% acrylamide [50:1], 0.4% SDS, 35% glycerol, 115 mM glycine, 230mM Tris [pH 8.8], H_2O, 0.1% APS, 0.05% TEMED). Frozen samples (−20°C) were thawed in a 37°C water bath for 5–10 min. Upper and lower chamber running buffers were made fresh daily. Upper chamber running buffer contained 5× running buffer (100 mM Tris, 150 mM glycine) diluted to 1× running buffer with H_2O, 0.1% SDS, and 0.07% mercaptoethanol (MCE). Lower chamber running buffer contained 5× running buffer (50 mM Tris, 75 mM glycine) diluted to 1× running buffer with H_2O, and 0.05% SDS. A sample (2.7 µl) was added to each well, and electrophoresis modules were placed into a 7° C room to run at 70 v for 30 h.

After the 30-h run time, gels were washed 3 times for 5 min with distilled, deionized H_2O. Gels were stained with Imperial Protein Stain (Thermo Fisher Scientific, Waltham, MA, USA) for a minimum of 1 h with gentle shaking. Stained gels were washed with dd H_2O for 30 min with gentle shaking. After the initial wash, gels were washed again in fresh dd H_2O overnight with gentle shaking. Washed gels were imaged using the Bio-Rad GelDoc Go Imaging System (Bio-Rad, Hercules, CA, USA) and gels were analyzed using Image Lab Software (Version 6.1, Bio-Rad, Hercules, CA, USA) to determine the percent MHC-type of samples. Samples were analyzed in duplicate and values were averaged to determine the value (%) of MHC-1 (Type I fibers) and MHC-2 (Type II fibers) in each sample. The differing isoforms of Type-2 MHC did not adequately separate to quantify individually. Thus, only the percentage of Type I fibers is reported.

Soluble and insoluble protein carbonyl

Soluble and insoluble fractions of muscle were separated using the protocol of Rowe et al. (2004). Protein concentration of both soluble and insoluble fractions was determined using a BCA protein assay kit (Pierce micro-BCA- assay, Thermo Scientific, Waltham, MA, USA) using a bovine serum albumin (BSA) standard curve. Carbonyls on proteins of each fraction were used to evaluate oxidative damage in each fraction using the methods of Reznick and Packer (1994) and Rowe et al. (2004).

Two dilutions (6 mg/ml) were made for each sample, one treated with 2,4 dinitrophenylhyrozene (DNPH) and one blank treated with HCl. Four ml of 10 mM DNPH in 2 M HCl was added to each treated tube and 4 ml 2 M HCl was added to each tube designated as a blank. Samples were vortexed and placed into dark storage for a 1-h incubation with vortexing occurring at 15-min intervals. After incubation, 5 ml of 20% tricarboxylic acid (TCA) was added to each tube and samples were held at 4°C for 10 min. Samples were centrifuged using a benchtop centrifuge at 1000 × g for 8 min. After centrifugation (1000 × g for 8 min at 20°C) 4 ml of 10% TCA was added to each pellet, which was resuspended. Samples were centrifuged (1000 × g for 8 min at 20°C) pellets were washed 3 times with 50:50 ethyl alcohol:ethyl acetate. After the final wash, pellets were dissolved in 6 M Guanidine hydrochloride and incubated at 37°C for 10 min. Protein concentration was determined for final samples using a BCA protein assay as previously described. Carbonyl content was determined using the absorbance of DNPH-treated samples vs blanks at 360 nm on a Spectramax plus spectrophotometer (Molecular Devices, Sunnydale, CA, USA). Carbonyl content (nmol/mg protein) for both the soluble and insoluble fractions was calculated using the molar extinction coefficient for DNPH (22,000 $M^{-1}cm^{-1}$).

Metabolite determination

Extractions and residual metabolic components were completed via methods described in Bergmeyer (1974) modified to a 96-well format by Hammelman et al. (2003) with further modifications. Powdered tissue (1 g) was deproteinated with 4 ml of 2 M HCl. An aliquot (1 mL) was removed immediately for use in glycogen determination. The remaining samples were incubated at 4°C for 15 min before 85µl of 5.4 M potassium hydroxide for malate assays.

For glycogen determination, 200 µl of the sample was combined with 50 µl potassium hydroxide and 1 ml of amyloglucosidase (AGS) (13 mg/ml in 0.2 M acetate buffer; pH = 4.8) and incubated for 3 h at 37°C with inverting every hour. After incubation, 100 µl of 2M HCl was added to each tube to stop hydrolysis. Then, 40 µl of 5.4 M KOH was added to each tube to neutralize the sample. Samples were incubated for an additional 10 min at 4°C before being centrifuged at 30,000 × g for 20 min at 4°C. A 400 µl aliquot of supernatant was added to a combined with 200 µl of 150 mM adenosine triphosphate (ATP)/12 mM nicotinamide adenine dinucleotide phosphate (NADP) in 0.3 M triethanolamine, 3mM $MgSO_4$; pH = 7.5, and an additional 1.7 ml of 0.3 M triethanolamine buffer. Initial absorbance was read at 340 nm on a Spectramax plus 96-well plate reader (Molecular Devices, Sunnydale, CA, USA). Then, 40 µl of glucose-6-phosphate dehydrogenase (4 IU/sample) in 3.2 M ammonium sulfate and 40 µl of hexokinase (2 IU/sample) in 3.2 M ammonium sulfate were added to each reaction. Reactions were incubated at 20°C for 20 min. Absorbance was read at 340 nm on a 96-well plate reader. The increase in absorbance during incubation was used, along with a standard curve of glucose subjected to the same assay conditions, to calculate glycogen content. Glucose and glucose-6-phosphate concentration without AGS digestion were subtracted from overall glycogen content to determine the final glycogen content.

An additional extraction was completed utilizing 0.5 g of powdered tissue which was deproteinated with 10 ml of 2M HCl. Homogenates were incubated (4°C) for 15 min before being centrifuged at 30,000 × g for 20 min at 4°C. Supernatant was neutralized with 3.5 ml of 5.4 M KOH to an approximate pH of 7.0. These extracts were used for lactate, glucose, and glucose-6-phosphate measurement.

For glucose and glucose-6-phosphate, 400 µl of the sample was added to a glass tube and combined with 200 µl of 150 mM ATP, 12 mM NADP in 0.3 M triethanolamine, 3 mM $MgSO_4$; pH = 7.5 solution and 1.7 ml of 0.3 triethanolamine (TEA) buffer. Absorbance at 340 nm was determined on a Spectramax plus 96-well plate reader (Molecular Devices, Sunnydale, CA). Then, 40 µl of glucose-6-phosphate dehydrogenase (4 IU/sample) in 3.2 M ammonium sulfate was added to each reaction before incubation (20°C) for 20 min. A second absorbance reading was taken before 40 µl of hexokinase (2 IU/sample) in 3.2 M ammonium sulfate was added to each reaction, which was incubated (20°C) for 20 min, and then a final absorbance measurement was taken. The increase in absorbance during the first and second incubations was compared to standard curves of glucose-6-phosphate and glucose, respectively to calculate concentrations of each metabolite.

To measure lactate, 50 µl of extracted and neutralized sample was added to a glass tube and combined with 150 µl of 196 mM HCl 95 mM KOH solution, 200 µl of 45 mM NAD, and 3 ml of reaction buffer (0.4 M hydrazine, 0.5 M glycine, pH 9.0). Initial absorbance (340 nm) was recorded using Spectramax plus 96-well plate reader (Molecular Devices, Sunnydale, CA, USA). Then, 40 µl of lactate dehydrogenase (20 IU/ml suspension) was added and reactions were incubated at 25°C for 2 h, and then absorbance (340 nm) was recorded. Increase in absorbance was used in conjunction with a standard curve of lactate exposed to the same reaction to determine muscle lactate concentration.

To measure malate, 200 µl of sample was added to a glass tube and combined with 200 µl of 45 mM NAD and 3 ml of reaction buffer (0.4 M hydrazine, 0.5 M glycine, pH 9.0). Absorbance was measured at 340 nm on a Spectramax plus 96-well plate reader (Molecular Devices, Sunnydale, CA, USA). Then, 40 µl of malate dehydrogenase (40 IU/ml) was added to each reaction, which was incubated at 25°C for 2 h. After incubation, absorbance was read again at 340 nm. The increase in absorbance at 340 nm was compared to a standard curve to calculate muscle malate concentrations.

Statistical analysis

The carcasses included in the present experiment were selected based on non-invasive predictions of color stability and tenderness. The purpose of using these predictions was to create a sample set that was quite variable regarding both tenderness and color stability. The accuracy of these predictions was marginal, particularly those for color stability (data not shown), and not sufficient for use as a categorical fixed effect

for statistical analysis; however, the goal of obtaining variation in tenderness and color stability was met. The range in slice shear force after 12 d of aging was from 7.6 to 30.3 kg with a standard deviation of 4.7. After 26 d of aging, the range in slice shear force values was from 7.5 to 35.6 kg with a standard deviation of 3.9. Overall color change at 12 d postmortem ranged from 1.1 to 26.5 with a standard deviation of 7.2. At 26 d of aging, overall color change ranged from 0.7 to 28.2 with a standard deviation of 6.8.

Four color stability and tenderness attribute clusters were created using agglomerative hierarchical clustering using the factoextra package (Kassambara and Mundt, 2020) in R statistical software (R Core Team, 2019) to represent variation in color stability and tenderness. Clustering was done using all simulated retail display data as well as overall tenderness, slice shear force, desmin degradation, and sarcomere length. Data were scaled using the scale() function and the Euclidean distance matrix was calculated using the dist() function. Dendrograms were generated using the hclust() function. Thus, the 4 resulting clusters represented samples differing in color stability and tenderness attributes.

Data were analyzed as a split-plot design using the GLIMMIX function of SAS version 9.4 (SAS Institute Inc., Cary, NC, USA) with carcass serving as the whole plot experimental unit, the cluster as the whole plot treatment, carcass side serving as the split-plot experimental unit, and aging time as the split-plot treatment. Cluster, aging period, and their interaction were included as fixed effects in the model. Carcass nested within the collection trip was included as a random effect in the model.

Color stability data were analyzed as repeated measures including the squared and cubed terms for day of display to the model to describe trends in color change. Regression equations were generated for changes in color attributes throughout retail display using contrasts to determine intercept (d 0) values and β-coefficients and to describe color change occurring during simulated retail display. Orthogonal contrasts were used to make pair-wise comparisons when differences were indicated. The Kenward-Roger approximation was used to estimate degrees of freedom.

The PRINCOMP procedure of SAS was used to decompose color and tenderness attributes into principal components at both aging periods. Data used for principal component analysis included overall tenderness, slice shear force, desmin degradation, sarcomere length, nitric oxide metmyoglobin-reducing ability, and oxygen consumption. Additionally, CIE L^*, a^*, and b^* as well as hue angle, chroma, and overall color change determined on days 0 and 11 of simulated retail display were included. Pearson correlation coefficients were generated using the PROC CORR procedure of SAS between the resulting principal components and the remaining metabolic variables to create loadings for each metabolic variable. Sample score plots and variable loading plots were produced to determine relationships between attributes and metabolic data. Pearson correlation coefficients between color, tenderness, and muscle metabolic characteristics were determined using the PROC CORR procedure in SAS. A level of $\alpha < 0.05$ was used for all judgments of statistical significance.

Results

Data collected across 2 aging times were used to segment carcasses into clusters based on exhibited color stability and tenderness characteristics. To aid in the interpretation of cluster comparisons, general descriptors of the color and tenderness profile for each cluster grouping are presented in Table 1. These descriptors are based on statistical differences observed across clusters described below. Carcasses included in cluster 1 were characterized as tender with moderate color stability attributes. Carcasses included in cluster 2 were considered tender and color stable. Carcasses classified in cluster 3 were considered tough and color labile. Carcasses in cluster 4 were characterized as moderate in tenderness and color stability. Further analyses included using these clusters along with aging time as fixed effects to ascertain the contribution of metabolic traits to tenderness and color stability.

A cluster by aging time interaction occurred for overall tenderness, nitric oxide metmyoglobin-reducing ability, carbonyls on proteins in the myofibrillar (insoluble fraction), and residual lactate concentration (Table 2). Overall tenderness scores increased for all

Table 1. Descriptors of cluster groupings based on agglomerative hierarchical clustering of beef longissimus muscles color stability and tenderness attributes of beef *longissimus lumborum* steaks at 2 aging periods

Cluster group	*n*	Descriptors
Cluster 1	29	Tender with moderate color stability
Cluster 2	38	Tender and color stable
Cluster 3	14	Tough and color labile
Cluster 4	15	Moderate tenderness and color stability

Table 2. Least-squares means (SEM) of metabolic and muscle characteristics of beef *longissimus lumborum* steaks in 4 clusters aged for 12 or 26 d

	12 d				26 d				
Variable	Cluster 1	Cluster 2	Cluster 3	Cluster 4	Cluster 1	Cluster 2	Cluster 3	Cluster 4	*P* value
Overall tenderness	6.18^{bcd}	5.84^{de}	4.80^{f}	5.61e	6.74^{a}	6.37^{b}	5.87^{cde}	6.31^{bc}	0.01
	(0.14)	(0.12)	(0.20)	(0.19)	(0.14)	(0.12)	(0.20)	(0.19)	
Nitric oxide metmyoglobin-reducing ability, %	69.56^{a}	51.61^{b}	54.78^{b}	52.73b	42.20^{c}	45.79^{bc}	41.60^{c}	45.51^{bc}	<0.001
	(2.74)	(2.39)	(3.94)	(3.81)	(2.74)	(2.39)	(3.94)	(3.81)	
Carbonyls in myofibrillar fraction, μmol/mg	3.80^{a}	2.27^{b}	3.94^{a}	3.06^{ab}	3.47^{a}	3.65^{a}	3.45^{a}	3.57^{a}	<0.01
	(0.34)	(0.30)	(0.49)	(0.47)	(0.34)	(0.30)	(0.49)	(0.47)	
Lactate, μmol/g	160.73^{a}	144.57^{b}	150.16^{ab}	149.09^{ab}	143.65^{b}	146.45^{b}	146.75^{b}	138.66^{b}	<0.01
	(3.71)	(3.24)	(5.33)	(5.15)	(3.76)	(3.24)	(5.33)	(5.15)	

$^{a–f}$Values within a row lacking a common superscript differ ($P < 0.05$).

clusters with increasing aging time ($P = 0.01$). At both aging times, *longissimus lumborum* steaks in cluster 3 had lower ($P < 0.05$) overall tenderness ratings than steaks from the other clusters; however, the increase in overall tenderness ratings with additional aging to 26 d postmortem was greater in steaks from cluster 3 than those from other clusters. Values for nitric oxide metmyoglobin-reducing ability decreased ($P < 0.05$) with increased aging time for steaks included in clusters 1 and 3. No differences across aging times existed in nitric oxide metmyoglobin-reducing ability values for steaks from clusters 2 and 4. Values for nitric oxide metmyoglobin-reducing ability were greater for steaks in cluster 1 at 12 d than in steaks from all the other cluster aging time combinations; however, after 26 d of aging, nitric oxide metmyoglobin-reducing ability did not differ across clusters. Carbonyl formation in the myofibrillar fraction increased ($P < 0.05$) substantially for cluster 2 with increasing aging time. No other differences in myofibrillar carbonyl content ($P > 0.05$) were found among clusters at either aging time. At 12 d postmortem, lactate content was greater ($P < 0.05$) in steaks from cluster 1 than in steaks from cluster 2. Lactate decreased ($P < 0.05$) substantially between day 12 and day 26 for cluster 1. By 26 d of aging, lactate concentration was similar ($P > 0.05$) across all clusters.

Changes in a^* during simulated retail display were indicative of the changes in other traits and are shown to represent the color stability of steaks across the clusters and aging times (Table 3, Figure 1). The statistical differences in the β-coefficients for the regression equations describing the change in a^* values during simulated retail display are shown in Table 3. Plots of the curves associated with these equations are shown in Figure 1. Initial a^* values on day 0 of simulated retail display did not differ ($P = 0.93$) across aging times or clusters (Table 3). The linear terms of the regression equations did not differ ($P = 0.23$) across clusters; however, the quadratic and cubic terms differed across clusters (Table 3). The differences in regression equations are difficult to interpret, so the regression curves were

Table 3. Regression coefficients (SE) for the change in a^* during simulated retail display in beef *longissimus lumborum* steaks in 4 clusters aged for 12 or 26 d

Cluster	Aging time	β0[1]	β1[2]	β2[3]	β3[4]
Cluster 1	12	33.69	1.32	−3.41^{ab}	−0.07^{bc}
		(0.46)	(1.22)	(2.35)	(1.32)
Cluster 2	12	33.32	4.65	−6.65^{b}	1.83^{b}
		(0.40)	(1.06)	(2.05)	(1.16)
Cluster 3	12	33.75	0.60	−3.94^{ab}	−2.58^{c}
		(0.66)	(1.75)	(3.38)	(1.90)
Cluster 4	12	33.53	5.99	−10.50^{bc}	3.33^{ab}
		(0.63)	(1.69)	(3.26)	(1.84)
Cluster 1	26	33.27	−2.87	1.18^{a}	−2.77^{c}
		(0.46)	(1.22)	(2.35)	(1.32)
Cluster 2	26	33.20	3.06	−6.40^{b}	1.91^{b}
		(0.40)	(1.06)	(2.05)	(1.16)
Cluster 3	26	33.35	2.40	−15.90^{c}	6.58^{a}
		(0.66)	(1.75)	(3.38)	(1.90)
Cluster 4	26	33.78	2.67	−6.37^{ab}	0.87^{bc}
		(0.63)	(1.69)	(3.26)	(1.84)
P > *F*		0.93	0.23	0.03	0.003

[1]β-coefficient for the intercept of the regression equation describing change in a^* values during simulated retail display.

[2]β-coefficient for the linear term of the regression equation describing change in a^* values during simulated retail display.

[3]β-coefficient for the quadratic term of the regression equation describing change a^* values during simulated retail display.

[4]β-coefficient for the cubic term of the regression equation describing change a^* values during simulated retail display.

$^{a–c}$β-coefficients within a column and attribute lacking a common superscript differ ($P < 0.05$).

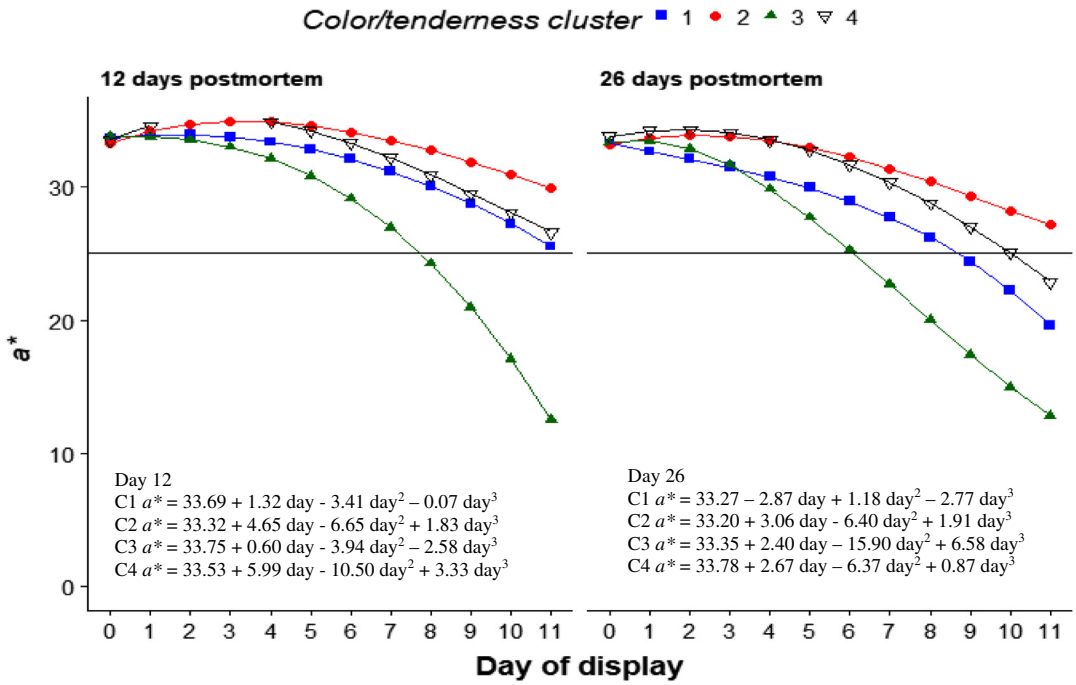

Figure 1. Change in *a** reflectance values over the duration of retail display for 4 cluster groups at 2 different aging periods. Equations for the change in *a** of steaks from each cluster at each aging time are shown.

plotted in Figure 1. Decreases in *a** values were more rapid and more extensive in steaks from cluster 3 than in steaks from other clusters at both aging times. Conversely, steaks from cluster 2 exhibited less change in *a** values during simulated retail display than steaks from other clusters. After 12 d of aging, steaks from cluster 1 and cluster 4 had similar stability of *a** values, which were intermediate to those of cluster 2 and cluster 3. After 26 d of aging, steaks from clusters 1 and 4 exhibited greater decreases in *a** values compared to the 12-d aging time. Additionally, steaks from cluster 4 had a lesser change in *a** during simulated retail display than those from cluster 1 after 26 d of aging.

Least-squares means for the cluster main effects on tenderness and metabolic traits are presented in Table 4. Slice shear force values were higher ($P < 0.0001$) for steaks in cluster 3 than all other groups. Sarcomere length was greater in steaks included in cluster 1 ($P = 0.01$) than those in clusters 3 and 4. Desmin degradation was greater ($P = 0.01$) in steaks from clusters 1 and 2 than those from clusters 3 and 4, indicating increased proteolysis for clusters 1 and 2. Myoglobin concentration was greater ($P < 0.0001$) in clusters 3 and 4 than in clusters 1 and 2. At 2 d postmortem, pH did not differ ($P < 0.05$) across clusters; however, ultimate pH (at 12- or 26-d postmortem) values were greater ($P = 0.003$) in cluster 4 than in clusters 1 and 2. Additionally, ultimate pH values were higher ($P = 0.003$) for steaks in both clusters 2 and 3 than those in cluster 1; however, the magnitude of these pH differences was small. Concentrations of glucose and glucose-6-phosphate did not differ across clusters. Malate concentration was greater ($P < 0.05$) in steaks from clusters 2 and 4 than in steaks from cluster 1, with malate concentration being intermediate in steaks from cluster 3. Steaks from clusters 3 and 4 had a greater proportion of MHC isoform-I than steaks from cluster 2.

Least-squares means for the aging time main effects on tenderness and metabolic traits of *longissimus lumborum* steaks are presented in Table 5. Increased aging time had a substantial impact on tenderness attributes on steaks from the *longissimus lumborum.* Slice shear force values decreased ($P < 0.0001$) as aging time increased. Sarcomere length ($P = 0.003$) and percent desmin degradation ($P < 0.0001$) were greater after 26 d of aging in comparison to 12 d. Myoglobin concentration was greater ($P = 0.03$) in steaks aged 26 d than those aged 12 d. Glycogen and glucose-6-phosphate concentrations were greater ($P < 0.002$) in steaks aged 12 d than those aged 26 d. Conversely, glucose concentration was lower ($P < 0.0001$) in steaks aged 12 d than in steaks aged 26 d. No differences ($P > 0.05$) in malate concentration, oxygen consumption, ultimate pH, sarcoplasmic carbonyls, or MHC isoforms were detected across aging times.

Table 4. Least-squares means (SEM) of muscle biochemical and metabolic attributes of beef *longissimus lumborum* steaks in 4 color tenderness groups

Variable	Cluster 1	Cluster 2	Cluster 3	Cluster 4	$P > -F$
Slice shear force, kg	12.41[b]	13.49[b]	18.57[a]	13.65[b]	<0.0001
	(0.61)	(0.53)	(0.88)	(0.85)	
Sarcomere length, µm	1.76[a]	1.74[ab]	1.71[b]	1.72[b]	0.01
	(0.01)	(0.01)	(0.01)	(0.01)	
Desmin degraded, %	91.88[a]	93.27[a]	86.60[b]	86.70[b]	0.01
	(1.48)	(1.30)	(2.13)	(2.06)	
Myoglobin, mg/g	3.98[b]	3.92[b]	5.01[a]	5.33[a]	<0.0001
	(0.12)	(0.10)	(0.17)	(0.16)	
Oxygen consumption, %	34.03	33.17	37.44	39.24	0.25
	(1.73)	(1.51)	(2.49)	(2.40)	
Day 2 pH	5.50	5.53	5.51	5.53	0.55
	(0.01)	(0.01)	(0.01)	(0.01)	
Ultimate pH	5.51[c]	5.53[b]	5.54[ab]	5.56[a]	0.003
	(0.01)	(0.01)	(0.01)	(0.01)	
Sarcoplasmic carbonyls, µmol/mg	1.47	1.76	1.54	1.44	0.30
	(0.14)	(0.12)	(0.20)	(0.18)	
Glycogen, µmol/g	13.90	11.29	14.95	14.35	0.37
	(1.52)	(1.33)	(2.19)	(2.11)	
Glucose, µmol/g	8.94	8.18	8.62	8.37	0.35
	(0.32)	(0.28)	(0.46)	(0.45)	
Glucose-6-phosphate, µmol/g	7.65	7.21	7.52	6.59	0.33
	(0.35)	(0.30)	(0.50)	(0.49)	
Malate, µmol/g	0.80[b]	1.03[a]	0.86[ab]	1.09[a]	0.05
	(0.06)	(0.05)	(0.09)	(0.09)	
MHC-Type I, %	31.08[ab]	30.29[b]	31.99[a]	31.84[a]	0.01
	(0.35)	(0.30)	(0.50)	(0.48)	

[a,b]Values within a row lacking a common superscript differ ($P < 0.05$).

Table 5. Least-squares means (SEM) of muscle biochemical and metabolic attributes of beef *longissimus lumborum* steaks aged for 12 or 26 d

Variable	12	26	SEM	$P > F$
Slice shear force, kg	15.90[a]	13.16[b]	0.44	<0.0001
Sarcomere length, µm	1.72[b]	1.75[a]	0.01	0.003
Desmin degraded, %	84.80[b]	94.42[a]	1.06	<0.0001
Myoglobin, mg/g	4.52[b]	4.60[a]	0.04	0.03
Oxygen consumption, %	35.64	36.30	1.16	0.55
Day 2 pH	5.51	5.52	0.01	0.16
Ultimate pH	5.53	5.54	0.01	0.20
Sarcoplasmic carbonyls, µmol/mg	1.55	1.55	0.10	0.99
Glycogen, µmol/g	14.67[a]	12.58[b]	0.97	0.002
Glucose, µmol/g	7.31[b]	9.74[a]	0.23	<0.0001
Glucose-6-phosphate, µmol/g	8.07[a]	6.41[b]	0.23	<0.0001
Malate, µmol/g	0.95	0.97	0.04	0.65
MHC-Type I, %	31.42	31.18	0.23	0.23

[a,b]Values within a row lacking a common superscript differ ($P < 0.05$).

Correlation coefficients between color and tenderness attributes with biochemical and metabolic attributes at 12 d of aging are presented in Table 6. Nitric oxide metmyoglobin-reducing ability exhibited no relationships ($P > 0.05$) with any color attributes in steaks aged 12 d of aging; however, sarcomere length was positively related to nitric oxide metmyoglobin-ability whereas desmin degradation was negatively related to nitric oxide metmyoglobin-reducing ability. Oxygen consumption of steaks aged for 12 d of aging was negatively related to L^* and a^* color values at the beginning of simulated retail display. By day 11 of simulated display, oxygen consumption was still negatively related to L^* values, but not a^* values. Oxygen consumption was negatively related to tenderness as indicated by an inverse relationship to overall tenderness ratings and a positive relationship to slice shear force values. Myoglobin concentration had strong inverse relationships to L^* values at the beginning and end of simulated retail display. Myoglobin concentration was positively related to a^* at the start of simulated retail display, but by day 11, myoglobin concentration was negatively related a^*. Myoglobin concentration was negatively related to overall tenderness scores and desmin degradation. Muscle pH values at 2 d postmortem were negatively related to L^* values at the onset of simulated retail display. Additionally, day 2 pH values values were positively correlated to slice shear force values at 12 d of aging. Ultimate pH values were negatively related to L^* and a^* values at day 0 of simulated display. After 11 d of simulated retail display, only a negative relationship with L^* remained for ultimate pH. No relationships ($P > 0.05$) between pHu and tenderness attributes at 12 d of aging were present in this study.

Glycogen concentration was negatively related to a^* values at 11 d of simulated display and SSF values and positively related to overall tenderness ratings in steaks aged for 12 d. Residual glucose was positively related to a^* values (0.35) at day 0 of retail display. A positive relationship existed between glucose concentration and overall tenderness ratings, whereas a negative relationship with SSF was also present at 12 d of aging. Relationships between color and tenderness attributes for residual glucose-6-phosphate followed the same trends as residual glucose. No relationships ($P > 0.05$) were found between residual lactate concentrations and any color or tenderness attributes of beef *longissimus lumborum* steaks aged for 12 d in the current study. Malate concentration was not ($P > 0.05$) related to any color attributes at day 0 of simulated retail display; however, malate concentration was

Table 6. Correlation coefficients for color and tenderness attributes with metabolic and biochemical attributes in beef *longissimus lumborum* steaks aged 12 d

Variable	*L** 0 d	*a** 0 d	*L** 11 d	*a** 11 d	Overall tenderness	Slice shear force	Desmin degraded	Sarcomere length
Nitric metmyoglobin-reducing ability	0.18	0.03	0.08	0.08	0.02	0.11	−0.21[a]	0.40[c]
Oxygen consumption	−0.33[b]	−0.42[c]	−0.26[b]	−0.02	−0.26[b]	0.26[a]	−0.07	−0.05
Myoglobin concentration	−0.81[c]	0.23[a]	−0.79[c]	−0.35[b]	−0.28[b]	0.09	−0.22[a]	−0.18
Day 2 pH	−0.24[a]	−0.19	−0.18	−0.02	−0.11	0.23[a]	−0.10	−0.05
Ultimate pH	−0.44[c]	−0.22[a]	−0.39[c]	−0.05	−0.10	0.12	−0.07	−0.14
Sarcoplasmic carbonyls	0.00	−0.05	0.11	0.02	−0.11	0.15	−0.15	−0.01
Myofibrillar carbonyls	−0.08	0.04	−0.11	−0.24[a]	0.05	0.02	0.06	−0.07
Glycogen	0.05	0.16	−0.01	−0.26[a]	0.25[a]	−0.28[b]	0.16	0.04
Glucose	0.18	0.35[b]	0.11	−0.03	0.20[a]	−0.24[a]	0.09	0.15
Glucose-6-phosphate	0.19	0.35[a]	0.14	−0.09	0.20[a]	−0.24[a]	0.15	0.13
Lactate	0.03	0.06	−0.08	−0.05	0.03	−0.12	−0.11	0.11
Malate	0.05	−0.06	0.15	0.29[b]	0.19	−0.23[b]	0.17	0.14
MHC-Type I,	−0.36[b]	0.10	−0.35[b]	−0.24[a]	0.00	−0.01	−0.07	0.01

[a]$P < 0.05$.

[b]$P < 0.01$.

[c]$P < 0.0001$.

Table 7. Correlation coefficients for color and tenderness attributes with metabolic and biochemical attributes in beef *longissimus lumborum* steaks aged 26 d

Variable	*L** 0 d	*a** 0 d	*L** 11 d	*a** 11 d	Overall tenderness	Slice shear force	Desmin degraded	Sarcomere length
Nitric metmyoglobin-reducing ability	−0.09	−0.20[a]	−0.08	0.17	−0.29[b]	0.06	0.05	−0.01
Oxygen consumption	−0.43[c]	−0.28[b]	−0.35[b]	−0.10	−0.13	0.25[a]	0.03	−0.12
Myoglobin concentration	−0.86[c]	0.41[c]	−0.77[c]	−0.25[a]	−0.28[b]	0.23[a]	−0.11	−0.13
Day 2 pH	−0.30[b]	−0.25[a]	−0.24[a]	−0.08	−0.28[b]	0.32[b]	−0.02	−0.01
Ultimate pH	−0.44[c]	−0.03	−0.32[b]	0.15	−0.29[b]	0.22[a]	0.15	0.07
Sarcoplasmic carbonyls	0.03	0.08	0.06	0.18	0.04	0.05	−0.05	−0.12
Myofibrillar carbonyls	0.15	−0.20	0.21[a]	0.09	0.18	−0.05	0.13	0.03
Glycogen	−0.01	0.10	−0.08	−0.05	0.31[b]	−0.30[b]	−0.05	0.01
Glucose	0.04	0.22[a]	0.04	−0.17	0.35[b]	−0.40[c]	−0.06	0.07
Glucose-6-phosphate	0.13	0.22[a]	0.14	−0.14	0.28[b]	−0.26[b]	0.00	−0.12
Lactate	−0.01	0.20[a]	−0.06	0.05	0.08	−0.09	0.01	0.03
Malate	−0.10	0.07	−0.05	0.20	−0.04	0.08	0.11	−0.19
MHC-Type I,	−0.31[b]	0.18	−0.24[a]	−0.22[a]	0.04	0.00	0.17	−0.02

[a]$P < 0.05$.

[b]$P < 0.01$.

[c]$P < 0.0001$.

positively related to *a** values on day 11 of simulated retail display. Moreover, malate and slice shear force were inversely related. The proportion of Type I fibers was negatively related *L** values on day 0 and day 11 of simulated retail display. Additionally, increased proportions of Type I fibers were associated with lesser *a** values on day 11 of simulated retail display.

Correlation coefficients between color and tenderness traits and metabolic and biochemical attributes at 26 d of aging are presented in Table 7. Nitric oxide metmyoglobin-reducing ability was negatively related to *a** values at the onset of simulated retail display as well as overall tenderness ratings. Oxygen consumption was negatively related to both *L** and at the onset of retail display. Additionally, oxygen consumption was negatively related to *L** values on day 11 of retail display and positively related to slice shear force values. Myoglobin concentration was negatively related to *L** values at both day 0 and day 11 of simulated retail display. On day 0 of display, myoglobin concentration was positively related to *a** values but by day 11 of display, that relationship was negative. Myoglobin

concentration was positively related to slice shear force values and negatively related to overall tenderness ratings after 26 d of aging. Values for pH on day 2 postmortem were negatively related to L^* and a^* values at day 0 of simulated display. On day 11 of simulated retail display, day 2 pH values were negatively related to L^* values. Additionally, muscle pH measured on day 2 postmortem was negatively related to overall tenderness ratings and positively related to slice shear force values. Ultimate pH values were negatively associated with L^* values on both day 0 and day 11 of simulated retail display. Values for ultimate pH were negatively related to overall tenderness ratings and positively related to slice shear force values. No relationships ($P > 0.05$) between carbonyl content in the soluble fraction and any color or tenderness traits were present after 26 d of aging. Carbonyl content in the insoluble fraction was positively related to L^* values at day 11 of retail display. Residual glycogen, glucose, and glucose-6-phosphate were positively related overall tenderness ratings and negatively related to slice shear force values. Glucose, glucose-6-phosphate, and lactate were positively related to a^* values on day 0 of simulated retail display. No relationships were detected between malate and any color or tenderness traits at 26 d of aging. The proportion of Type I fibers was negatively related to L^* values at day 0 and day 11 of simulated display. Additionally, the proportion of Type I fibers was negatively related to a^* values on day 11 of display.

Results of the principal component analysis of tenderness and color stability traits at 12 d of aging are presented in Figure 2A. The principal component analysis included color variables at the beginning and end of simulated retail display as well as nitric oxide metmyoglobin-reducing ability collected at both aging times. Additionally, the analysis included overall tenderness ratings, slice shear force, desmin degradation, and sarcomere length. Loadings for the remaining metabolic variables were derived to ascertain their relationships to tenderness and color stability traits. Component 1 explained 28.8% of the variation and was largely indicative of color stability. Negative loadings for component 1 were associated with overall color change and hue angle measured at the end of simulated retail display. Conversely, positive loadings for component 1 were associated with higher values for a^*, b^*, and chroma measured at the end of simulated retail display. Positive loadings for component 2 were associated with greater a^*, b^*, and chroma measured at the initiation of display. Initial hue angle values and L^* values measured at the beginning and end of simulated retail display had positive loadings for both components 1 and 2.

Loadings for overall tenderness were similar to those for the initial hue angle measured at the beginning of simulated retail display and loadings for slice shear force were negative for both component 1 and component 2. Loadings for desmin degradation were along component 1, indicating some relationship to lower values for a^* and b^* at the end of simulated display. Moreover, loadings for oxygen consumption were relatively close to those for slice shear force values.

Muscle pH measured at 2 d postmortem and at the end of aging was associated with negative loadings for component 2. Moreover, muscle pH was closely related to oxygen consumption and nitric oxide metmyoglobin-reducing ability after 26 d of aging. We have previously reported strong relationships among reducing ability, oxygen consumption, and muscle pH in a sample set widely divergent in muscle pH (King et al., 2024). In that report, we speculated that increased muscle pH provided an environment more favorable for the mitochondrial function required for oxygen consumption and reducing ability. The pH range in the present experiment is much smaller than in our previous report; however, the strong relationship between these traits was evident. Loadings for glycogen, glucose, and glucose-6-phosphate were close together and associated with positive values for component 2. Increased myoglobin concentration was strongly associated with greater color change during simulated retail display.

Generally, loadings were similar for variables across aging times; however, the loadings for nitric oxide metmyoglobin-reducing ability were quite different after increased aging. After 12 d of aging, nitric oxide metmyoglobin-reducing ability had a positive loading for component 2; however, after 26 d of aging, reducing ability had a negative loading from component 2 and was much more closely related to ultimate pH in steaks aged for 26 d of aging. This is consistent with the notion that increased muscle pH helps to maintain the ability of mitochondria to respire in aged muscle. After 12 d of aging, malate concentration was strongly related to desmin degradation and had a positive loading for component 1; however, after 26 d of aging, malate's loading was not closely related to either component. Similarly, carbonyls on proteins in the myofibrillar fraction were not related to either component after 26 d of aging, but at 12 d of aging, myofibrillary carbonyl content was associated with negative loadings for component 1 very similar to those for the proportion of Type I muscle fibers. Thus, at 12 d postmortem, myofibrillar carbonyl content was associated with greater color change during simulated retail display and reduced overall tenderness ratings.

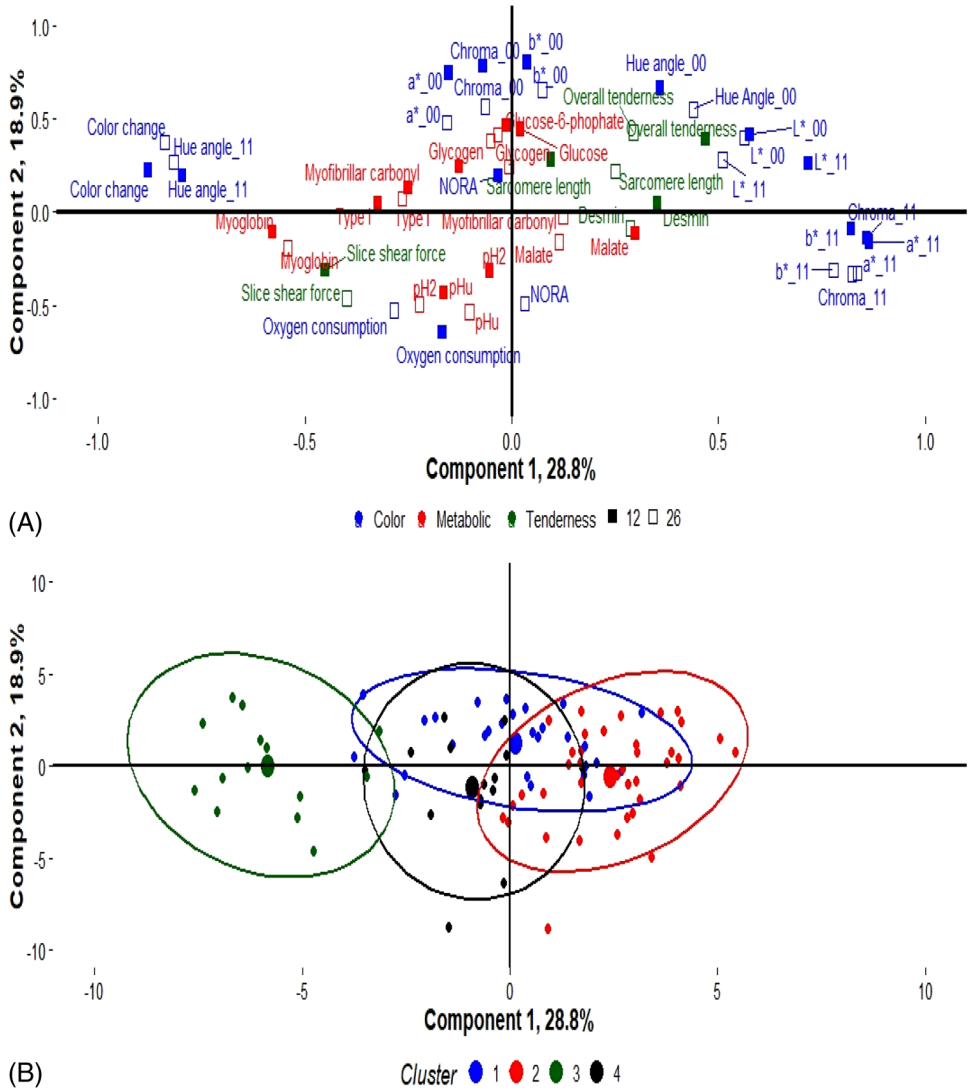

Figure 2. A) Principal component analysis loadings of color and tenderness attributes and metabolic traits of beef *longissimus lumborum* steaks aged for 12 or 26 d. B) Score plot for cluster groupings.

Sample scores for the cluster groupings of samples included in the principal component analysis are shown in Figure 2B. These clusters are primarily segmented along component 1. Cluster 3, which exhibited lesser tenderness and lesser color stability than the other 3 clusters, had the most negative loadings for component 1. Cluster 2 had the greatest loadings for component 1. The scores for individuals included in clusters 1 and 4 had a substantial amount of overlap with regard to component 1, but muscles included in cluster 1 tended to have higher loadings for component 2 than those included in cluster 4.

Discussion

Substantial resources have been dedicated to understanding the mechanisms responsible for biological variation in both meat tenderness and color stability; however, numerous gaps exist in the understanding of the biochemical regulation of these traits, and few investigations have delved into both these economically important traits simultaneously. Recent advancements have provided new insight into metabolic factors contributing to variation in both traits. These studies have indicated the importance of the glycolytic pathway and mitochondrial function to tenderness (Antonelo et al., 2020; Carlson et al., 2017; King et al., 2019; Santos et al., 2016) and color stability (Canto et al., 2015, Nair et al., 2018, Ramanathan et al., 2019) variation. Because similar pathways are implicated in regulating both traits, it is important to understand interrelationships in the mechanisms to avoid unintended consequences of selection and management.

Our observations on the phenotypic relationship between tenderness and color stability have been mixed. In large populations of cattle that have been managed similarly (i.e., the USMARC Germplasm Evaluation population described by Ahlberg et al. [2016]), the correlation between slice shear force and overall color change is moderately negative over numerous calf-crops and harvest days ([$r = -0.21$; $n = 10{,}000$], D. A. King, unpublished data); however, in sample sets collected under commercial conditions across production lots (i.e., different feedyard pens), correlations between slice shear force and overall color change during simulated retail display range from moderately negative to moderately positive (D. A. King, unpublished data). Our hypothesis regarding these observations is that some inherent antagonisms exist between color stability and tenderness; however, numerous ante and postmortem management practices are beneficial for both traits, whereas others are deleterious for both traits. Thus, in some sample sets across production lots, positive relationships exist between tenderness and color stability. Carcasses were selected on 6 production days, spanning 3 calendar months for the current experiment from a commercial facility and the correlation between overall color change and slice shear force was 0.14 (data not shown).

Selection criteria for the present experiment were intended to maximize variation in tenderness and lean color stability of *longissimus lumborum* so that the relationships between these meat quality end points and metabolic factors could be ascertained. Sufficient variation existed in these muscles to examine the relationships between tenderness and color stability. Agglomerative hierarchical clustering was used to segregate the muscles sampled for this experiment into clusters with similar color stability and tenderness characteristics within each cluster. Contrasts of metabolic traits across these clusters, coupled with correlations between the metabolic and quality traits and multivariate results enabled an understanding of the contributions of muscle metabolism to meat tenderness and color stability.

Clustering identified groups of *longissimus lumborum* muscles that were generally consistent with the overall correlation between tenderness and lean color stability. Moreover, the principal component analysis identified relationships between tenderness and color traits at the beginning and the end of simulated retail display. Component traits that are understood to directly contribute to tenderness and color stability exhibited relationships to the other trait. Oxygen consumption and nitric oxide metmyoglobin-reducing ability are generally used as component traits to explain variations in color stability; however, in the present experiment, nitric oxide metmyoglobin-reducing ability was negatively correlated to overall tenderness in *longissimus lumborum* steaks aged for 26 d and desmin degradation in steaks aged for 12 d. Increased oxygen consumption was associated with increased slice shear force values at both aging times. The principal component analysis indicated that increased desmin degradation was associated with lower values of a^*, b^*, and chroma at the end of simulated retail display. Previously, Wulf et al. (1997) reported negative correlations between measures of lean color at grading and Warner-Bratzler shear force and proposed using lean color to augment the USDA quality grading standard (Wulf and Page, 2000).

Collectively, the results of the present experiment indicate a negative impact of increased oxidative metabolism on both tenderness and color stability. As noted previously, cluster 3 exhibited lesser tenderness attributes and more labile lean color attributes than the other clusters. This cluster comprised muscles with the most negative loadings for component 1 in the principal component analysis. Negative loadings for component 1 were also associated with increased myoglobin concentration, increased proportion of Type I fibers, and, in steaks aged for 12 d, increased carbonyls on myofibrillar proteins. This suggests that muscles with more oxidative metabolism are less tender and have less lean color stability. It is notable that cluster 4, which had moderate tenderness and color stability characteristics, was less extreme in relation to component 1 but still tended to have negative loadings for that component. It is also notable that cluster 3 did not differ ($P > 0.05$) from cluster 4 for any of the metabolic factors measured in the present experiment. Thus, it is apparent metabolic factors impact these traits, but the metabolic factors measured in the present experiment contributed but were not entirely causative of this variation.

Muscle metabolism has long been understood to impact both tenderness and color stability, even if the mechanisms have not been fully understood. Muscle pH is commonly used to characterize muscle metabolism. Increasing the rate and extent of pH decline, within the normal range, has been reported to improve tenderness (Eilers et al., 1996; Jones and Tatum, 1994) and lean color (Zhang et al., 2018). In the present experiment, increased muscle pH measured at 2 d postmortem or the end of aging had a weak, negative relationship to both tenderness and color stability.

Historically, the role that muscle fiber type plays in meat tenderness has not been totally understood. Many

studies have indicated that more oxidative fibers, or Type I fibers, are more tender than their more glycolytic counterparts as oxidative fibers are more susceptible to oxidative stress, which can lead to apoptosis occurring at earlier time points than glycolytic fibers (Picard et al., 2018; Picard et al., 2014). Antonelo et al. (2020) found that tender beef underwent oxidative stress at an earlier time point than tough beef. In the current study, little relationship was evident between the proportion of Type I fibers and tenderness; however, as noted earlier, nitric oxide metmyoglobin-reducing ability and oxygen consumption, which are indicative of mitochondrial function, contributed to variation in tenderness traits. Moreover, the concentration of myoglobin, which stores oxygen until needed by mitochondria, was negatively related to tenderness traits.

Increased oxygen consumption, associated with more Type I fibers, has been implicated in decreased color stability (McKenna et al., 2005; Sammel et al., 2002). This is consistent with the results of the present experiment. In this study, total myoglobin concentration was negatively related to color attributes by day 11 of simulated retail display. This is consistent with previous reports that suggest beef longissimus muscles with greater glycolytic metabolism possessed greater lean color stability than those with more oxidative metabolism (Canto et al., 2015; King et al., 2010).

Chauhan et al. (2019) reported that even in the presence of excess glycogen, oxidative muscle fibers exhibited less glycolytic flux and consequently had lesser concentrations of glucose, glucose-6-phosphate, and lactate compared to more glycolytic muscle fibers. In the present study, increased concentrations of glucose and glucose-6-phosphate were associated with greater a^*, b^*, and chroma values at the beginning of display and improved overall tenderness ratings. King et al. (2019) also detected strong negative relationships between glucose and glucose-6-phosphate and slice shear force values. Antonelo et al. (2020) reported a negative correlation between glucose and Warner-Bratzler shear force values and that lactate was implicated in differentiating between tender and tough *longissimus thoracis muscles.*

Scheffler et al. (2015) indicated that mitochondria can delay pH decline in an in vitro system by diverting lactate to the TCA cycle. The malate–aspartate shuttle functions to transport electrons from the sarcoplasm to the mitochondria to undergo electron transport. In the present study, malate was associated with greater oxidative metabolism. Malate concentration was greatest in steaks from cluster 1, which was also the cluster with the greatest overall tenderness ratings. Moreover, in *longissimus lumborum* steaks aged for 12 d, malate was positively correlated to a^* values at the end of display and negatively correlated to slice shear force. Both the correlation analysis and principal component analysis indicated that malate concentration played a greater role in influencing tenderness and color stability characteristics after 12 d of aging than at 26 d of aging. The potential for malate to benefit lean color stability, particularly at shorter aging times, may be a result of greater production of reducing equivalents in the early postmortem environment. In contrast to the present experiment, King et al. (2019) reported a strong positive relationship between malate and slice shear force and a negative relationship between malate and desmin degradation in a metabolomics study. Moreover, Santos et al. (2016) found greater concentrations of malate dehydrogenase in tough *longissimus lumborum* steaks than in their tender counterparts.

Conclusion

Data from this study indicate that variation in color stability and tenderness in the *longissimus lumborum* at 2 different aging times was impacted by metabolic characteristics. Relationships existed among tenderness measures, color stability measures, and their component traits. Increased oxidative metabolism was associated with decreases in both tenderness and lean color stability. Many of the metabolic variables measured in this experiment were selected because of previous reports of their potential for use as biomarkers. These variables were helpful in characterizing metabolic differences contributing to variation in tenderness and lean color stability. More work is warranted to fully elucidate the metabolic regulation of tenderness and lean color stability. Moreover, more work is needed to fully understand the interrelationships between these economically important meat quality traits in order to devise strategies that benefit both traits.

Acknowledgments

Mention of trade names or commercial products in this publication is solely for the purpose of providing specific information and does not imply recommendation or endorsement by the U.S. Department of Agriculture. The authors are grateful to Megan Landes-Murphy, Kristen Ostdiek, and Casey Trambly of the U.S. Meat Animal Research Center for their assistance in the execution of this experiment and to Jody

Gallagher of the U.S. Meat Animal Research Center for her secretarial assistance. USDA is an equal opportunity provider and employer.

Author Contribution

J.V. Cooper contributed to data curation, methodology, data analysis, writing, and original draft preparation. D. A. King contributed conceptualization, investigation supervision, data curation, methodology, data analysis, writing, and editing. S.D. Shackelford contributed to conceptualization, methodology, reviewing, and editing. P. Ekeren, contributed to data curation, methodology, and editing. C.L. Lorenzen contributed to methodology and editing. T.L. Wheeler contributed to conceptualization, reviewing, and editing.

Literature Cited

Ahlberg, C. M., L. A. Kuehn, R. M. Thallman, S. D. Kachman, W. M. Snelling, and M. L. Spangler. 2016. Breed effects and genetic parameter estimates for calving difficulty and birth weight in a multibreed population1. J. Anim. Sci. 94:1857–1864. https://doi.org/10.2527/jas.2015-0161

AMSA. 2016. Research guidelines for cookery, sensory evaluation, and instrumental tenderness measurements of meat. 2nd ed. Am. Meat Sci. Assoc. Champaign, IL.

Antonelo, D. S., N. R. B. Cônsolo, J. F. M. Gómez, M. Beline, R. S. Goulart, R. R. P. S. Corte, L. A. Colnago, M. W. Schilling, D. E. Gerrard, and S. L. Silva. 2020. Metabolite profile and consumer sensory acceptability of meat from lean Nellore and Angus × Nellore crossbreed cattle fed soybean oil. Food Res. Int. 132:109056. https://doi.org/10.1016/j.foodres.2020.109056

Bekhit, A. E., and C. Faustman. 2005. Metmyoglobin reducing activity. Meat Sci. 71:407–439. https://doi.org/10.1016/j.meatsci.2005.04.032

Bendall, J. R., editor. 1973. Postmortem changes in muscle. Academic Press, New York, NY

Bergmeyer, H. U., editor. 1974. Methods of enzymatic analysis. Academic Press, New York, NY

Canto, A. C., S. P. Suman, M. N. Nair, S. Li, G. Rentfrow, C. M. Beach, T. J. Silva, T. L. Wheeler, S. D. Shackelford, A. Grayson, R. O. McKeith, and D. A. King. 2015. Differential abundance of sarcoplasmic proteome explains animal effect on beef Longissimus lumborum color stability. Meat Sci. 102:90–98. https://doi.org/10.1016/j.meatsci.2014.11.011

Carlson, K. B., K. J. Prusa, C. A. Fedler, E. M. Steadham, E. Huff-Lonergan, and S. M. Lonergan. 2017. Proteomic features linked to tenderness of aged pork loins. J. Anim. Sci. 95:2533–2546. https://doi.org/10.2527/jas.2016.1122

Chauhan, S. S., M. N. LeMaster, D. L. Clark, M. K. Foster, C. E. Miller, and E. M. England. 2019. Glycolysis and pH decline terminate prematurely in oxidative muscles despite the presence of excess glycogen. Meat Muscle Biol. 3. https://doi.org/10.22175/mmb2019.02.0006

Cross, H. R., R. Moen, and M. S. Stanfield. 1978. Training and testing of judges for sensory analysis of meat quality. Food Technol. 32:48–54.

Cross, H. R., R. L. West, and T. R. Dutson. 1981. Comparison of methods for measuring sarcomere length in beef semitendinosus muscle. Meat Sci. 5:261–266. https://doi.org/10.1016/0309-1740(81)90016-4

D'Alessandro, A., C. Marrocco, S. Rinalducci, C. Mirasole, S. Failla, and L. Zolla. 2012. Chianina beef tenderness investigated through integrated Omics. J. Proteomics 75:4381–4398. https://doi.org/10.1016/j.jprot.2012.03.052

Eilers, J. D., J. D. Tatum, J. B. Morgan, and G. C. Smith. 1996. Modification of early-postmortem muscle pH and use of postmortem aging to improve beef tenderness. J. Anim. Sci. 74:790–798.

Gagaoua, M., V. Monteils, and B. Picard. 2019. Decision tree, a learning tool for the prediction of beef tenderness using rearing factors and carcass characteristics. J. Sci. Food Agr. 99:1275–1283. https://doi.org/10.1002/jsfa.9301

Grayson, A. L., S. D. Shackelford, D. A. King, R. O. McKeith, R. K. Miller, and T. L. Wheeler. 2016. The effects of degree of dark cutting on tenderness and sensory attributes of beef. J. Anim. Sci. 94:2583–2591. https://doi.org/10.2527/jas.2016-0388

Hammelman, J. E., B. C. Bowker, A. L. Grant, J. C. Forrest, A. P. Schinckel, and D. E. Gerrard. 2003. Early postmortem electrical stimulation simulates PSE pork development. Meat Sci. 63:69–77. https://doi.org/10.1016/s0309-1740(02)00057-8

Huff-Lonergan, E., T. Mitsuhashi, D. D. Beekman, F. C. J. Parrish, D. G. Olson, and R. M. Robson. 1996. Proteolysis of specific muscle structural proteins by mu-calpain at low pH and temperature is similar to degradation in postmortem bovine muscle. J. Anim. Sci. 74:993–1008.

Jones, B. K., and J. D. Tatum. 1994. Predictors of beef tenderness among carcasses produced under commercial conditions. J. Anim. Sci. 72:1492–1501. https://doi.org/10.2527/1994.7261492x

Joseph, P., S. P. Suman, G. Rentfrow, S. Li, and C. M. Beach. 2012. Proteomics of muscle-specific beef color stability. J. Agr. Food Chem. 60:3196–3203. https://doi.org/10.1021/jf204188v

Kassambara, A., and F. Mundt. 2020. Factoextra: extract and visualize the results of multivariate data analyses, R package version 1.0.7. https://CRAN.R-project.org/package=factoextra. (Accessed May 12, 2020).

King, D. A., M. E. Dikeman, T. L. Wheeler, C. L. Kastner, and M. Koohmaraie. 2003. Chilling and cooking rate effects on some myofibrillar determinants of tenderness of beef. J. Anim. Sci. 81:1473–1481. https://doi.org/10.2527/2003.8161473x

King, D. A., M. C. Hunt, S. Barbut, J. R. Claus, D. P. Cornforth, P. Joseph, Y. H. B. Kim, G. Lindahl, R. A. Mancini, M. N. Nair, K. J. Merok, A. Milkowski, A. Mohan, F. Pohlman, R. Ramanathan, C. R. Raines, M. Seyfert, O. Sørheim, S. P. Suman, and M. Weber. 2023. American Meat Science Association Guidelines for Meat Color Measurement. Meat Muscle Biol. 6. https://doi.org/10.22175/mmb.12473

King, D. A., R. K. Miller, R. O. McKeith, A. L. Grayson, S. D. Shackelford, K. B. Gehring, J. W. Savell, and T. L.

Wheeler. 2024. Multivariate examination of metabolic contributions to beef longissimus lumborum flavor. Meat Muscle Biol. 8:1–14. https://doi.org/10.22175/mmb.17055

King, D. A., S. D. Shackelford, C. D. Broeckling, J. E. Prenni, K. E. Belk, and T. L. Wheeler. 2019. Metabolomic investigation of tenderness and aging response in beef longissimus steaks. Meat Muscle Biol. 3:76–89. https://doi.org/10.22175/mmb2018.09.0027

King, D. A., S. D. Shackelford, L. A. Kuehn, C. M. Kemp, A. B. Rodriguez, R. M. Thallman, and T. L. Wheeler. 2010. Contribution of genetic influences to animal-to-animal variation in myoglobin content and beef lean color stability. J. Anim. Sci. 88:1160–1167. https://doi.org/10.2527/jas.2009-2544

King, D. A., S. D. Shackelford, A. B. Rodriguez, and T. L. Wheeler. 2011. Effect of time of measurement on the relationship between metmyoglobin reducing activity and oxygen consumption to instrumental measures of beef longissimus color stability. Meat Sci. 87:26–32. https://doi.org/10.1016/j.meatsci.2010.08.013

Koohmaraie, M. 1996. Biochemical factors regulating the toughening and tenderization processes of meat: Meat for the Consumer 42nd International Congress of MEAT Science and Technology. Meat Sci. 43:193–201. https://doi.org/10.1016/0309-1740(96)00065-4

Koohmaraie, M., M. P. Kent, S. D. Shackelford, E. Veiseth, and T. L. Wheeler. 2002. Meat tenderness and muscle growth: is there any relationship? Meat Sci. 62:345–352.

Maddock, K. R., E. Huff-Lonergan, L. J. Rowe, and S. M. Lonergan. 2005. Effect of pH and ionic strength on mu- and m-calpain inhibition by calpastatin. J. Anim Sci. 83:1370–1376. https://doi.org/10.2527/2005.8361370x

Malheiros, J. M., C. P. Braga, R. A. Grove, F. A. Ribeiro, C. R. Calkins, J. Adamec, and L. A. L. Chardulo. 2019. Influence of oxidative damage to proteins on meat tenderness using a proteomics approach. Meat Sci. 148:64–71. https://doi.org/10.1016/j.meatsci.2018.08.016

Mancini, R. A., and M. C. Hunt. 2005. Current research in meat color: 51st International Congress of Meat Science and Technology (ICoMST). Meat Sci. 71:100–121. https://doi.org/10.1016/j.meatsci.2005.03.003

McKeith, R. O., D. A. King, A. L. Grayson, S. D. Shackelford, K. B. Gehring, J. W. Savell, and T. L. Wheeler. 2016. Mitochondrial abundance and efficiency contribute to lean color of dark cutting beef. Meat Sci. 116:165–173. https://doi.org/10.1016/j.meatsci.2016.01.016

McKenna, D. R., P. D. Mies, B. E. Baird, K. D. Pfeiffer, J. W. Ellebracht, and J. W. Savell. 2005. Biochemical and physical factors affecting discoloration characteristics of 19 bovine muscles. Meat Sci. 70:665–682. https://doi.org/10.1016/j.meatsci.2005.02.016

Mitacek, R. M., Y. Ke, J. E. Prenni, R. Jadeja, D. L. VanOverbeke, G. G. Mafi, and R. Ramanathan. 2019. Mitochondrial degeneration, depletion of NADH, and oxidative stress decrease color stability of wet-aged beef longissimus steaks. J. Food Sci. 84:38–50. https://doi.org/10.1111/1750-3841.14396

Nair, M. N., S. Li, C. M. Beach, G. Rentfrow, and S. P. Suman. 2018. Changes in the sarcoplasmic proteome of beef muscles with differential color stability during postmortem aging. Meat Muscle Biol. 2:1–17. https://doi.org/10.22175/mmb2017.07.0037

Nair, M. N., S. P. Suman, M. K. Chatli, S. Li, P. Joseph, C. M. Beach, and G. Rentfrow. 2016. Proteome basis for intramuscular variation in color stability of beef semimembranosus. Meat Sci. 113:9–16. https://doi.org/10.1016/j.meatsci.2015.11.003

Page, J. K., D. M. Wulf, and T. R. Schwotzer. 2001. A survey of beef muscle color and pH. J. Anim. Sci. 79:678–687. https://doi.org/10.2527/2001.793678x

Picard, B., C. Barboiron, D. Chadeyron, and C. Jurie. 2011. Protocol for high-resolution electrophoresis separation of myosin heavy chain isoforms in bovine skeletal muscle. Electrophoresis 32:1804–1806. https://doi.org/10.1002/elps.201100118

Picard, B., M. Gagaoua, M. Al-Jammas, L. De Koning, A. Valais, and M. Bonnet. 2018. Beef tenderness and intramuscular fat proteomic biomarkers: muscle type effect. PeerJ 6: e4891. https://doi.org/10.7717/peerj.4891

Picard, B., M. Gagaoua, D. Micol, I. Cassar-Malek, J. F. Hocquette, and C. E. Terlouw. 2014. Inverse relationships between biomarkers and beef tenderness according to contractile and metabolic properties of the muscle. J. Agr. Food Chem. 62:9808–9818. https://doi.org/10.1021/jf501528s

R Core Team. 2019. R: A language and environmnent for statistical computing. https://www.R-project.org/. (Accessed April 10, 2020).

Ramanathan, R., F. Kiyimba, J. Gonzalez, G. Mafi, and U. DeSilva. 2020a. Impact of up- and downregulation of metabolites and mitochondrial content on pH and color of the longissimus muscle from normal-pH and dark-cutting beef. J. Agr. Food Chem. 68:7194–7203. https://doi.org/10.1021/acs.jafc.0c01884

Ramanathan, R., M. N. Nair, M. C. Hunt, and S. P. Suman. 2019. Mitochondrial functionality and beef colour: a review of recent research. S. Afr. J. Anim. Sci. 49. https://doi.org/10.4314/sajas.v49i1.2

Ramanathan, R., M. N. Nair, Y. Wang, S. Li, C. M. Beach, R. A. Mancini, K. Belskie, and S. P. Suman. 2021. Differential abundance of mitochondrial proteome influences the color stability of beef longissimus lumborum and psoas major muscles. Meat Muscle Biol. 5. https://doi.org/10.22175/mmb.11705

Ramanathan, R., S. P. Suman, and C. Faustman. 2020b. Biomolecular interactions governing fresh meat color in post-mortem skeletal muscle: a review. J. Agr. Food Chem. 68:12779–12787. https://doi.org/10.1021/acs.jafc.9b08098

Reznick, A. Z., and L. Packer. 1994. Oxidative damage to proteins: spectrophotometric method for carbonyl assay. In: Methods in enzymology. Academic Press, New York. p. 357–363. https://doi.org/10.1016/s0076-6879(94)33041-7

Rowe, L. J., K. R. Maddock, S. M. Lonergan, and E. Huff-Lonergan. 2004. Influence of early postmortem protein oxidation on beef quality. J. Anim. Sci. 82:785–793. https://doi.org/10.2527/2004.823785x

Sammel, L. M., M. C. Hunt, D. H. Kropf, K. A. Hachmeister, C. L. Kastner, and D. E. Johnson. 2002. Influence of chemical characteristics of beef inside and outside semimembranosus on

color traits. J. Food Sci. 67:1323–1330. https://doi.org/10.1111/j.1365-2621.2002.tb10282.x

Santos, C., E. Huff Lonergan, S. M. Lonergan, T. L. Wheeler, and S. D. Shackelford. 2016. Determination of protein markers for beef tenderness in U.S. Select beef. Paaper presented at: American Meat Science Association 69th Reciprocal Meat Conference, San Angelo, TX. June 19–22.

Scheffler, T. L., S. K. Matarneh, E. M. England, and D. E. Gerrard. 2015. Mitochondria influence postmortem metabolism and pH in an in vitro model. Meat Sci. 110:118–125. https://doi.org/10.1016/j.meatsci.2015.07.007

Shackelford, S. D., D. A. King, and T. L. Wheeler. 2012a. Chilling rate effects on pork loin tenderness in commercial processing plants. J. Anim. Sci. 90: 2842–2849. https://doi.org/10.2527/jas.2011-4855

Shackelford, S. D., T. L. Wheeler, D. A. King, and M. Koohmaraie. 2012b. Field testing of a system for online classification of beef carcasses for longissimus tenderness using visible and near-infrared reflectance spectroscopy. J. Anim. Sci. 90:978–988. https://doi.org/10.2527/jas.2011-4167

Shackelford, S. D., T. L. Wheeler, and M. Koohmaraie. 1999. Evaluation of slice shear force as an objective method of assessing beef longissimus tenderness. J. Anim. Sci. 77:2693–2699. https://doi.org/10.2527/1999.77102693x

Shackelford, S. D., T. L. Wheeler, and M. Koohmaraie. 2003. On-line prediction of yield grade, longissimus muscle area, preliminary yield grade, adjusted preliminary yield grade, and marbling score using the MARC beef carcass image analysis system. J. Anim. Sci. 81:150–155. https://doi.org/10.2527/2003.811150x

Suman, S. P., C. Faustman, S. L. Stamer, and D. C. Liebler. 2006. Redox instability induced by 4-hydroxy-2-nonenal in porcine and bovine myoglobins at pH 5.6 and 4 degrees C. J. Agr. Food Chem. 54:3402–3408. https://doi.org/10.1021/jf052811y

Suman, S. P., and P. Joseph. 2013. Myoglobin chemistry and meat color. Annu. Rev. Food Sci. T. 4:79–99. https://doi.org/10.1146/annurev-food-030212-182623

Tang, J., C. Faustman, T. A. Hoagland, R. A. Mancini, M. Seyfert, and M. C. Hunt. 2005. Postmortem oxygen consumption by mitochondria and its effects on myoglobin form and stability. J. Agr. Food Chem. 53:1223–1230. https://doi.org/10.1021/jf048646o

Taylor, R. C., G. H. Geesink, V. F. Thompson, M. Koohmaraie, and D. E. Goll. 1995. Is Z-disk degradation responsible for postmortem tenderization? J. Anim. Sci. 73:1351–1367.

United States Department of Agriculture (USDA). 2014. Institutional Meat Purchase Specifications Fresh Beef Series 100. https://www.ams.usda.gov/sites/default/files/media/IMPS_100_Fresh_Beef%5B1%5D.pdf. (Accessed May 3, 2018.)

Wang, Y., S. Li, G. Rentfrow, J. Chen, H. Zhu, and S. P. Suman. 2021. Myoglobin post-translational modifications influence color stability of beef longissimus lumborum. Meat Muscle Biol. 5. https://doi.org/10.22175/mmb.11689

Watanabe, A., C. C. Daly, and C. E. Devine. 1996. The effects of the ultimate pH of meat on tenderness changes during ageing. Meat Sci. 42:67–78. https://doi.org/10.1016/0309-1740(95)00012-7

Wheeler, T. L., S. D. Shackelford, and M. Koohmaraie. 1998. Cooking and palatability traits of beef longissimus steaks cooked with a belt grill or an open hearth electric broiler. J. Anim. Sci. 76:2805–2810. https://doi.org/10.2527/1998.76112805x

Wulf, D. M., S. F. O'Connor, J. D. Tatum, and G. C. Smith. 1997. Using objective measures of muscle color to predict beef longissimus tenderness. J. Anim. Sci. 75:684–692. https://doi.org/10.2527/1997.753684x

Wulf, D. M., and J. K. Page. 2000. Using measurements of muscle color, pH, and electrical impedance to augment the current USDA beef quality grading standards and improve the accuracy and precision of sorting carcasses into palatability groups. J. Anim. Sci. 78:2595–2607. https://doi.org/10.2527/2000.78102595x

Zhang, Y.-M., D. L. Hopkins, X.-X. Zhao, R. van de Ven, Y.-W. Mao, L.-X. Zhu, G.-X. Han, and X. Luo. 2018. Characterisation of pH decline and meat color development of beef carcasses during the early postmortem period in a Chinese beef cattle abattoir. J. Integr. Agr. 17:1691–1695. https://doi.org/10.1016/S2095-3119(17)61890-2